

Hyperbolic Anomaly Detection

CVPR (2024)

Huimin Li, Zhentao Chen, Yunhao Xu, Junlin Hu*

School of Software, Beihang University, Beijing, China



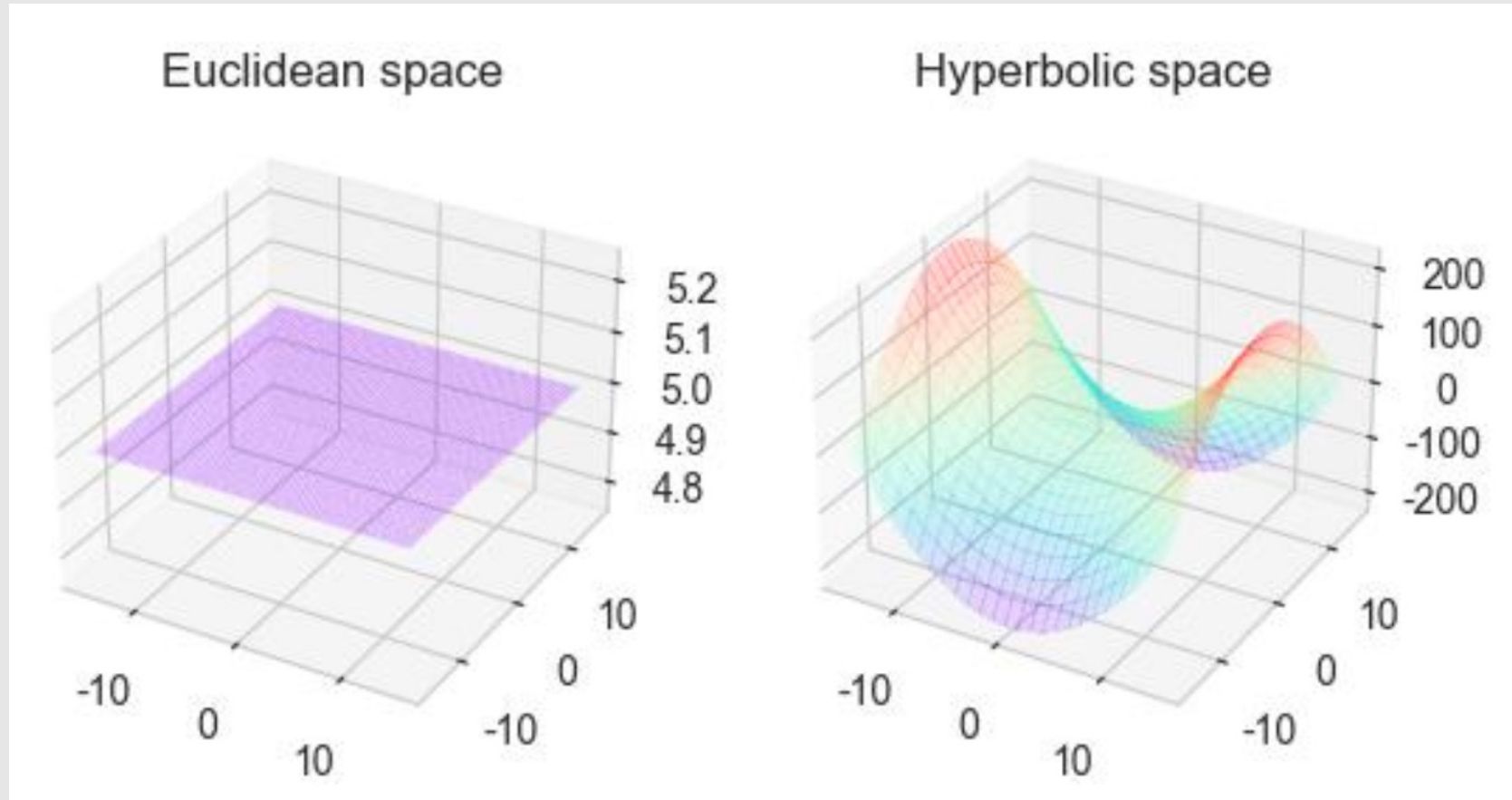
Jaemin Kim



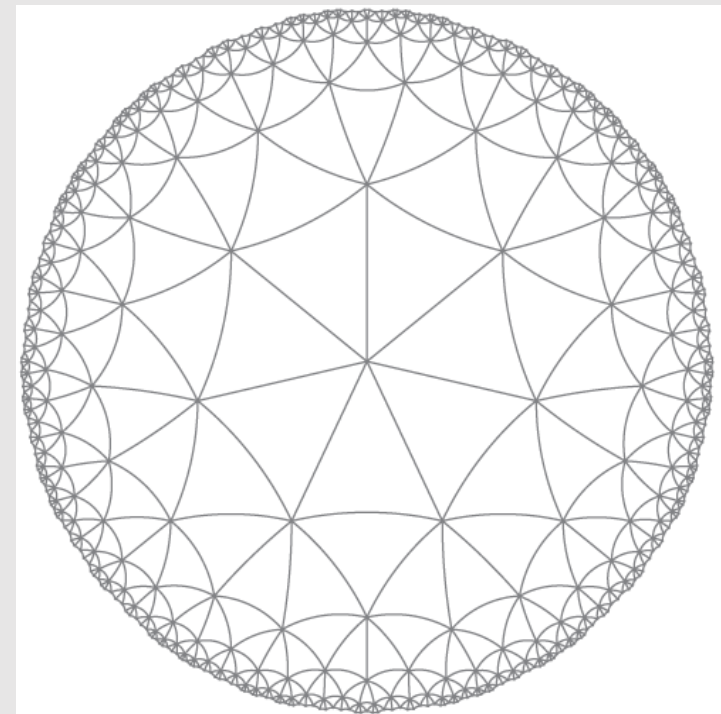
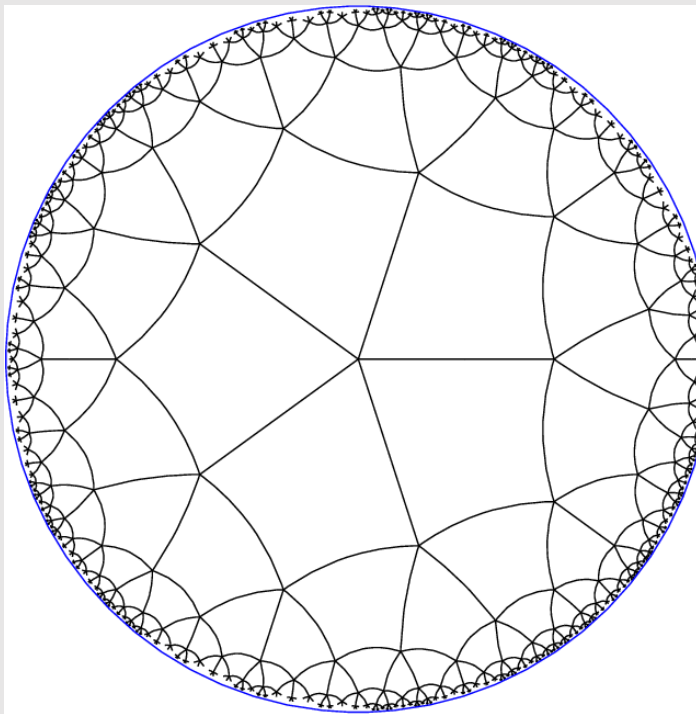
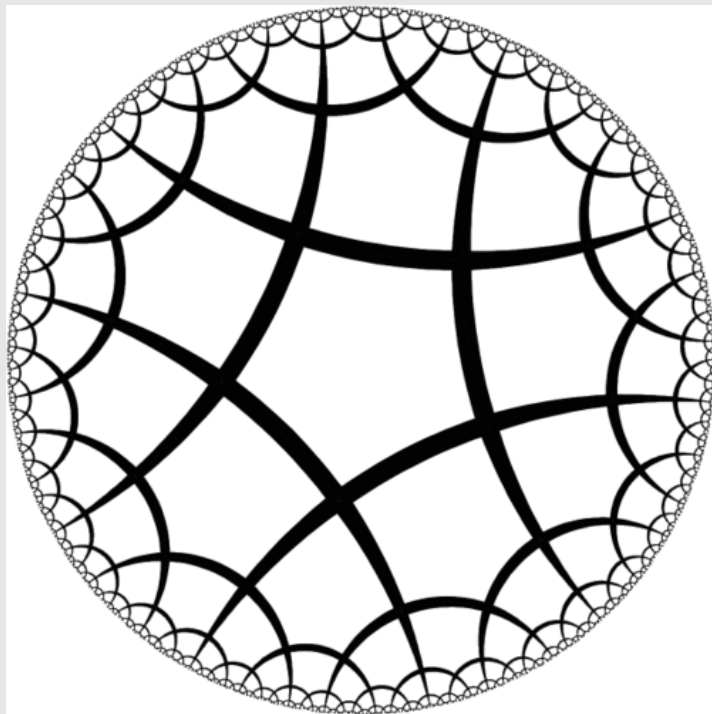
2025-10-31

- 1) Background**
- 2) Introduction & Related work**
- 3) HypAD**
- 4) Experiment & Result**
- 5) Conclusion & Discussion**

Euclidean Space & Hyperbolic Space



Hyperbolic Space



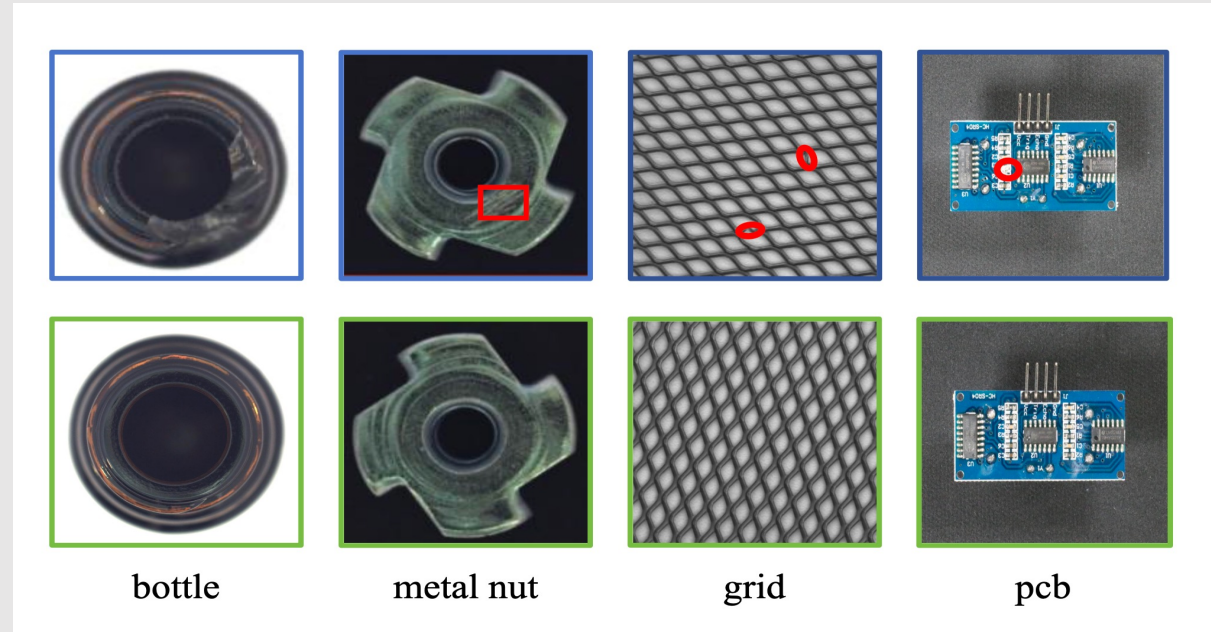
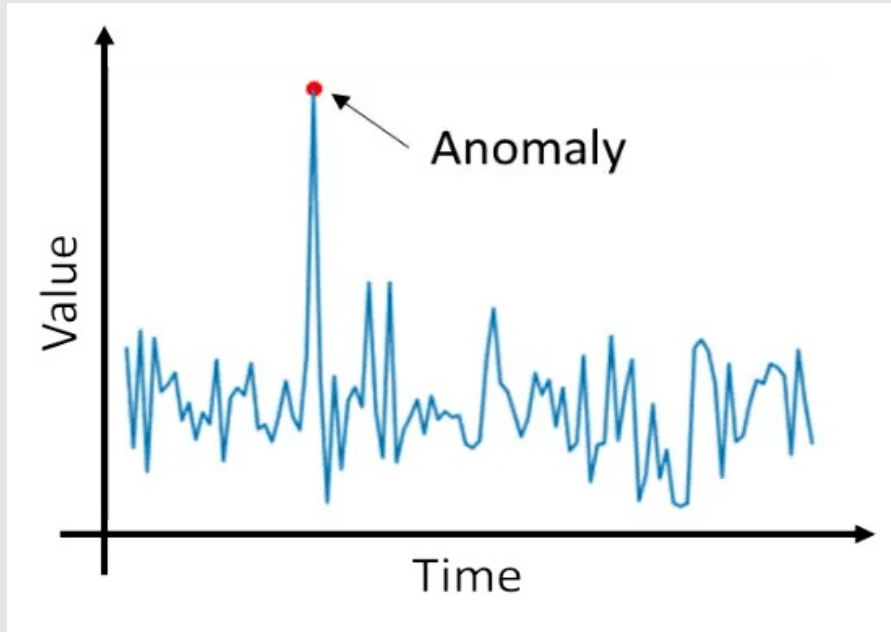
Hyperbolic Anomaly Detection

Hyperbolic Space

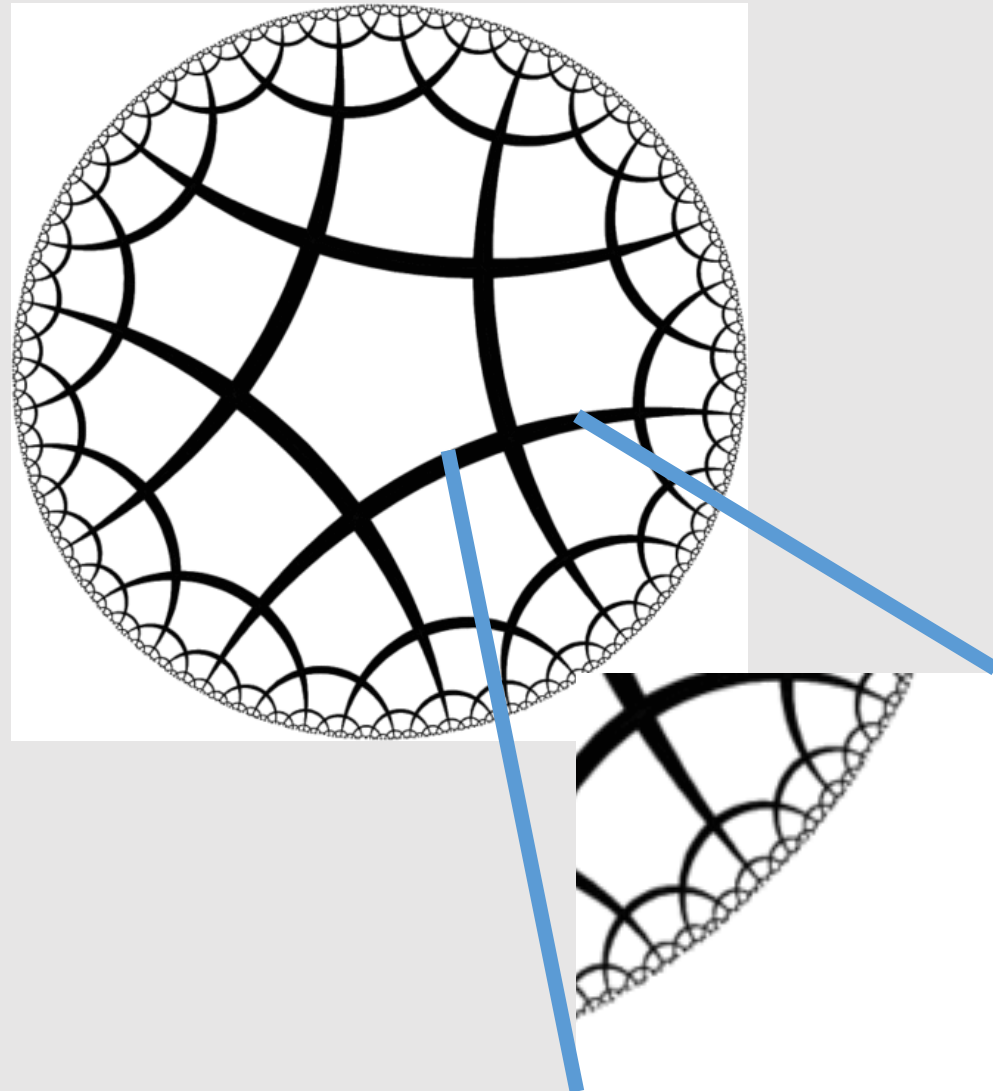
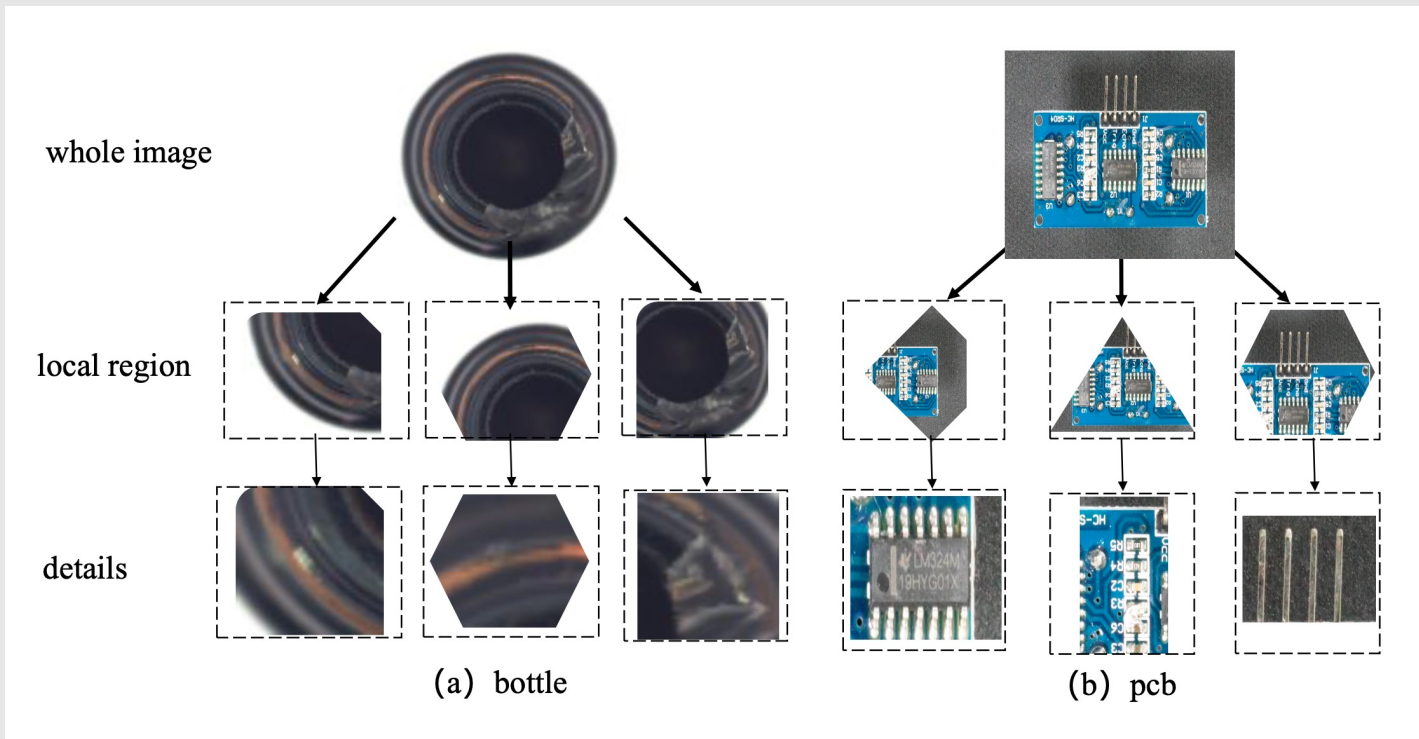


Hyperbolic Anomaly Detection

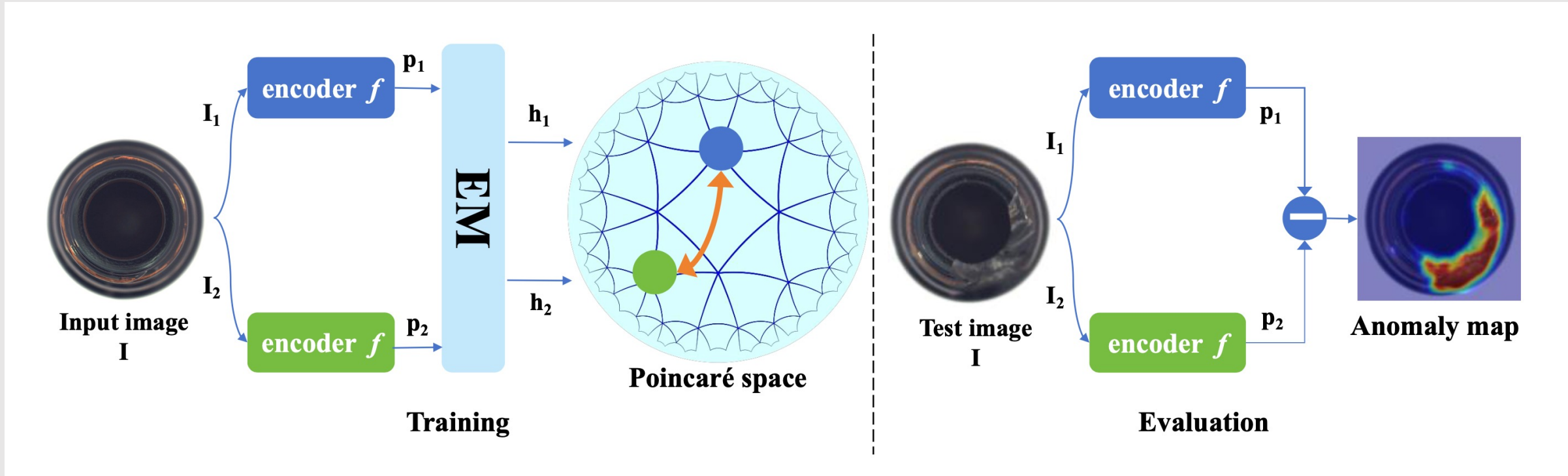
Anomaly Detection & Hyperbolic Space



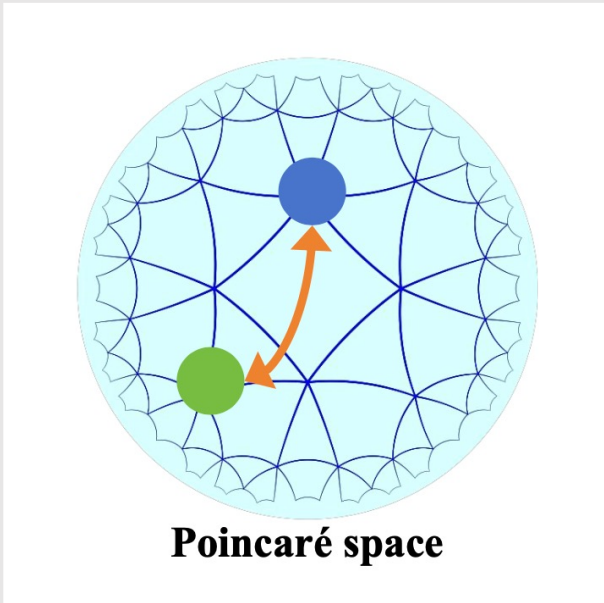
Hyperbolic Embeddings



Proposed Method - HypAD(Hyperbolic Anomaly Detection)



Hyperbolic Space



Poincare ball model $(\mathbb{D}_c^n, g^{\mathbb{D}})$

n-dimensional manifold $\mathbb{D}^n = \{x \in \mathbb{R}^n : c\|x\|^2 < 1\}$

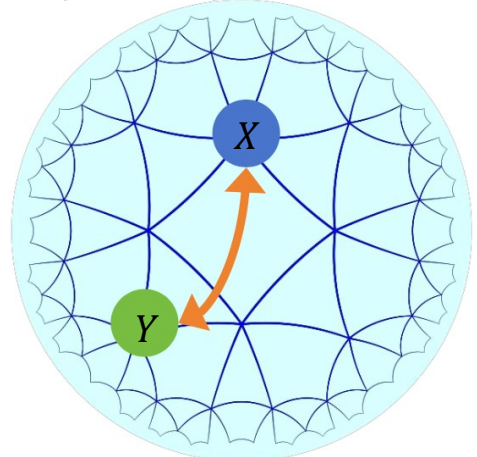
Riemannian metric $g^{\mathbb{D}} = \lambda_c^2 g^{\mathbb{E}}$

Conformal factor $\lambda_c = \frac{2}{1 - c\|x\|^2}$

Euclidean metric tensor $g^{\mathbb{E}} = I_n$

Hyperbolic Space

$$X \in \mathbb{D}_c^n, Y \in \mathbb{D}_c^n$$



Poincaré space

Poincare ball model $(\mathbb{D}_c^n, g^{\mathbb{D}})$ n -dimensional manifold $\mathbb{D}^n = \{x \in \mathbb{R}^n : c\|x\|^2 < 1\}$ Riemannian metric $g^{\mathbb{D}} = \lambda_c^2 g^{\mathbb{E}}$ Conformal factor $\lambda_c = \frac{2}{1 - c\|x\|^2}$ Euclidean metric tensor $g^{\mathbb{E}} = I_n$

$$\mathbf{x} \oplus_c \mathbf{y} = \frac{(1 + 2c\langle \mathbf{x}, \mathbf{y} \rangle + c\|\mathbf{y}\|^2)\mathbf{x} + (1 - c\|\mathbf{x}\|^2)\mathbf{y}}{(1 + 2c\langle \mathbf{x}, \mathbf{y} \rangle + c^2\|\mathbf{x}\|^2\|\mathbf{y}\|^2)}.$$

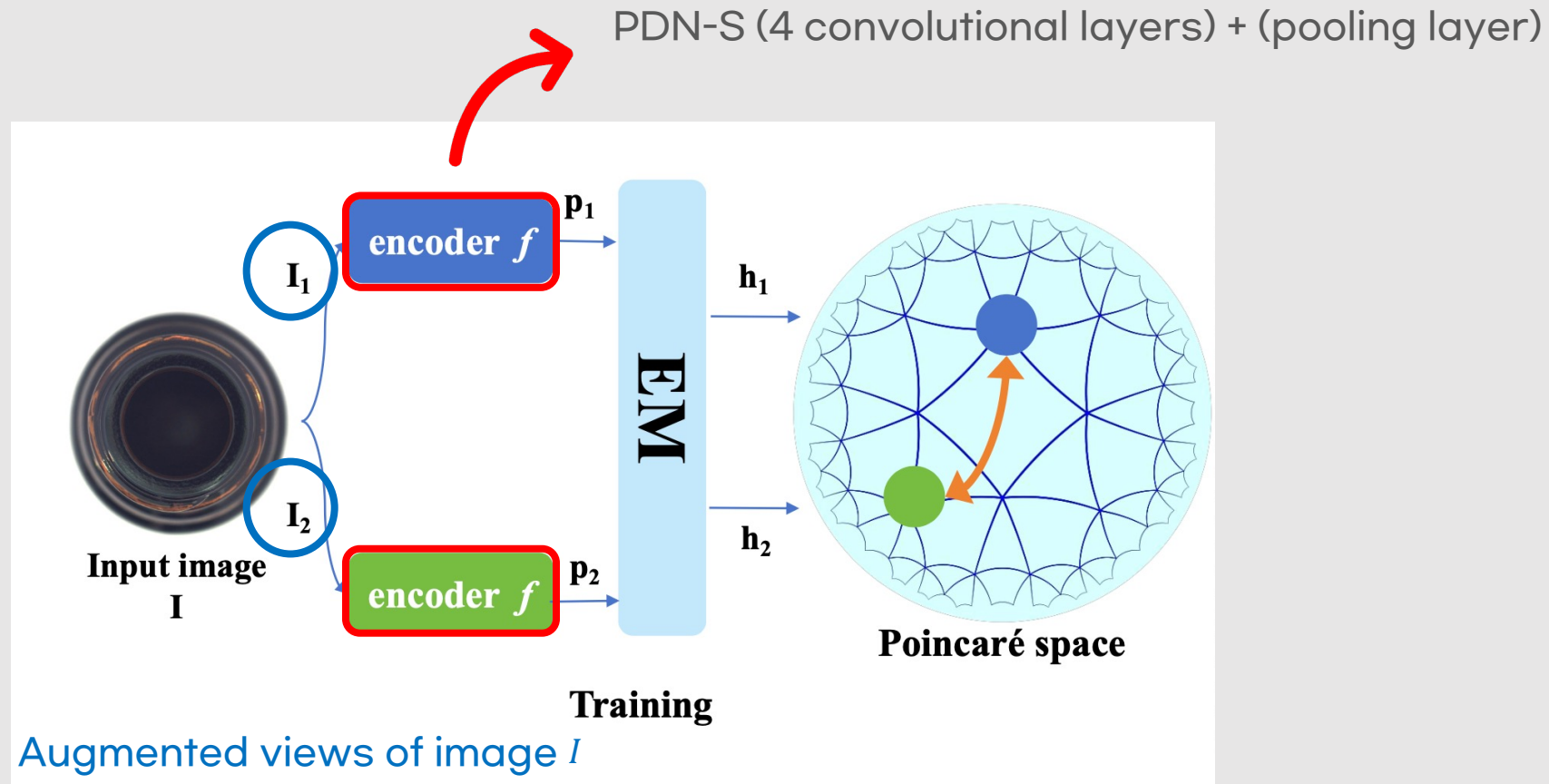
Addition

$$d_{\mathbb{H}}(\mathbf{x}, \mathbf{y}) = \frac{2}{\sqrt{c}} \operatorname{arctanh}(\sqrt{c}\|\mathbf{x} \oplus_c \mathbf{y}\|).$$

Distance

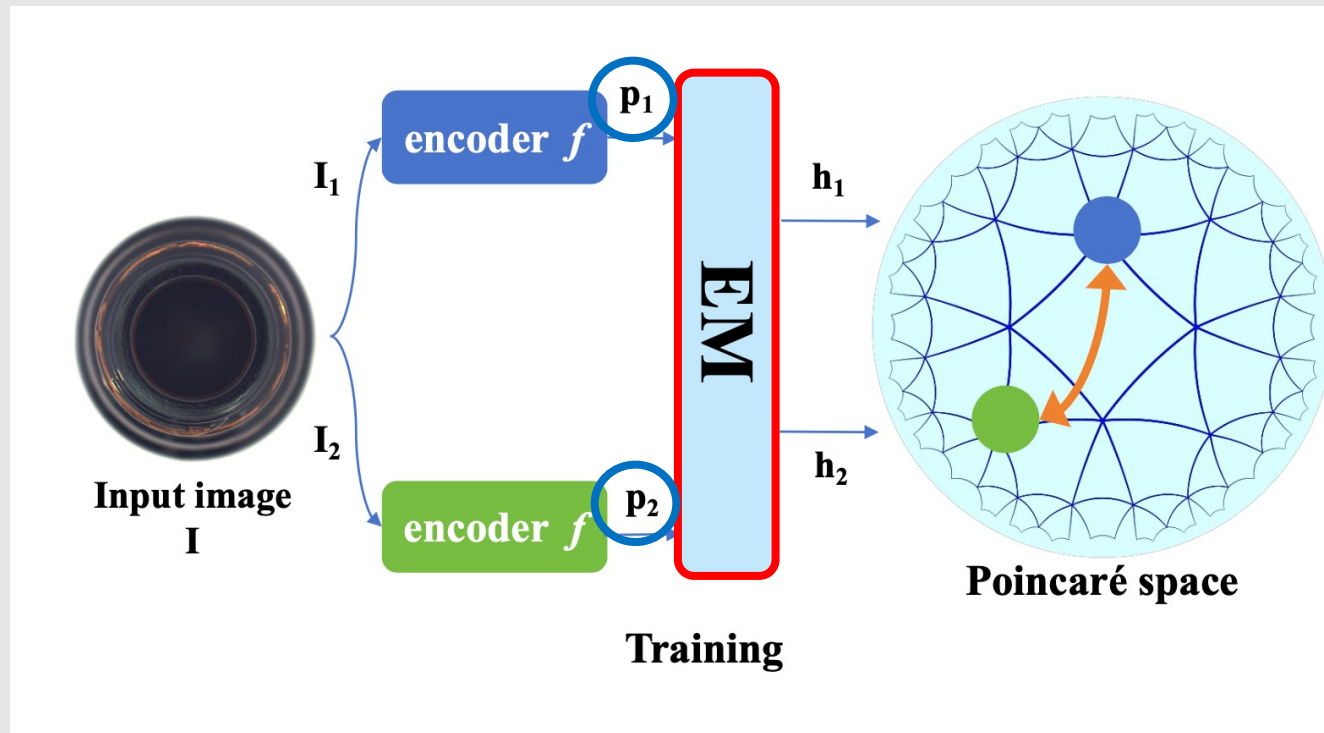
Hyperbolic Anomaly Detection

Backbone



Hyperbolic Anomaly Detection

EM Module (Exponential Mapping)

Euclidean space features P_1, P_2

Hyperbolic Anomaly Detection

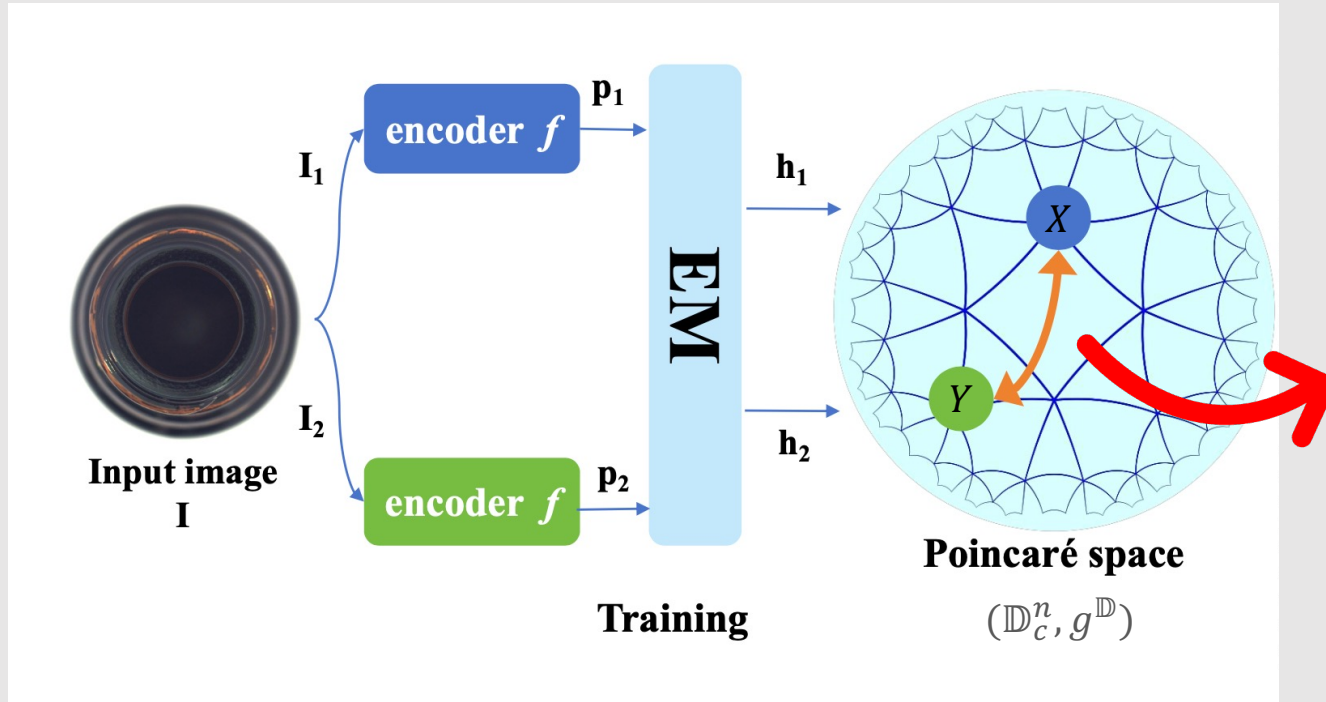
$$h_0 \in \mathbb{D}_c^n$$

$$h = \exp_{h_0}^c(p)$$

$$= h_0 \oplus_c (\tanh\left(\sqrt{c} \frac{\lambda_{h_0}^c \|p\|}{2}\right) \frac{p}{\sqrt{c}\|p\|})$$

Hyperbolic Anomaly Detection

Optimization



Loss Function

$$d_{\mathbb{H}}(h_1, h_2) = \frac{2}{\sqrt{c}} \operatorname{arctanh}(\sqrt{c} \| -h_1 \oplus_c h_2 \|)$$

c is the curvature parameter, h_1 and h_2 are image embeddings in hyperbolic(Poincare) space

Distance in Poincaré space

$$X \in \mathbb{D}_c^n, Y \in \mathbb{D}_c^n$$

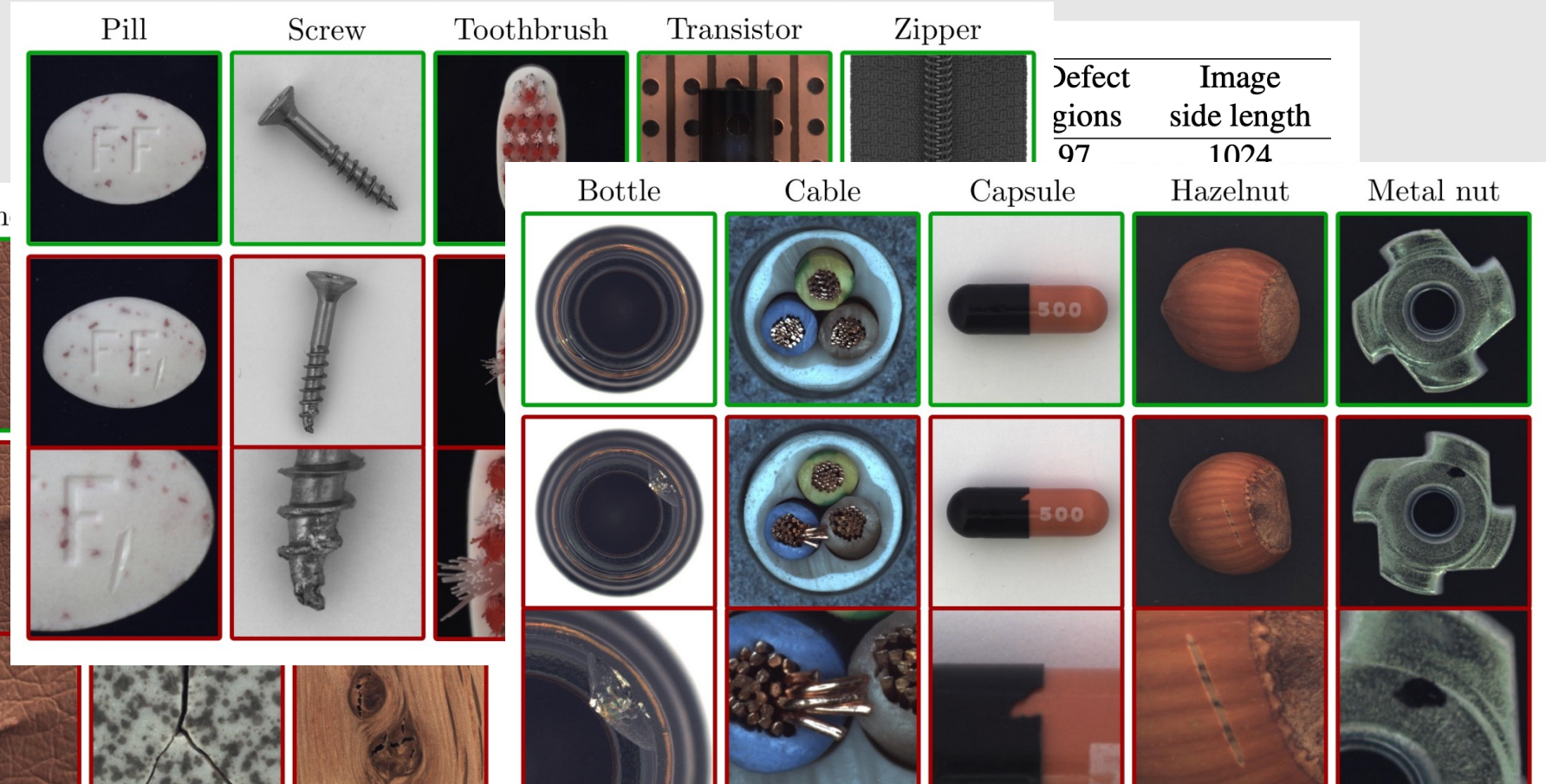
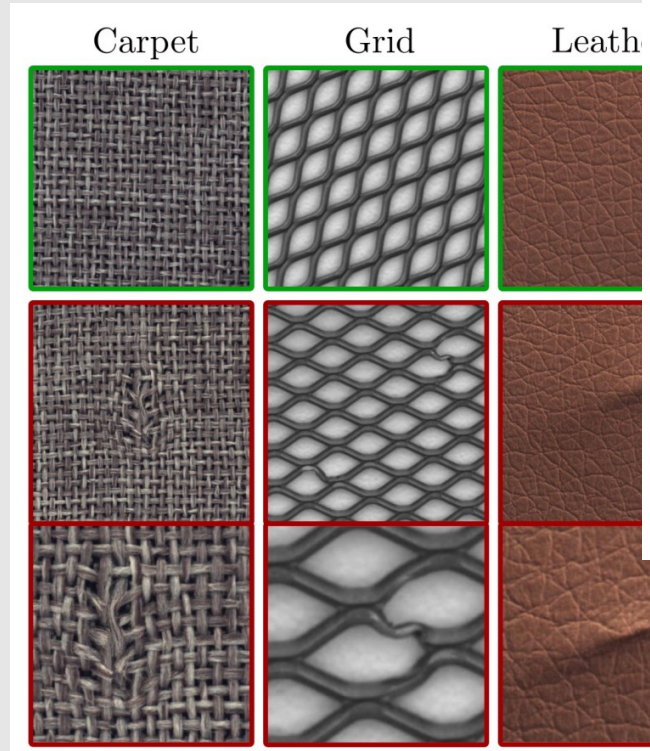
$$d_{\mathbb{H}}(X, Y) = \frac{2}{\sqrt{c}} \operatorname{arctanh}(\sqrt{c} \| -X \oplus_c Y \|)$$

Experiment & Result

GSPS

Datasets

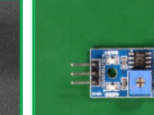
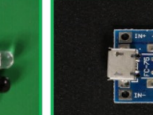
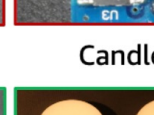
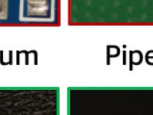
MVTec AD



Experiment & Result

Datasets

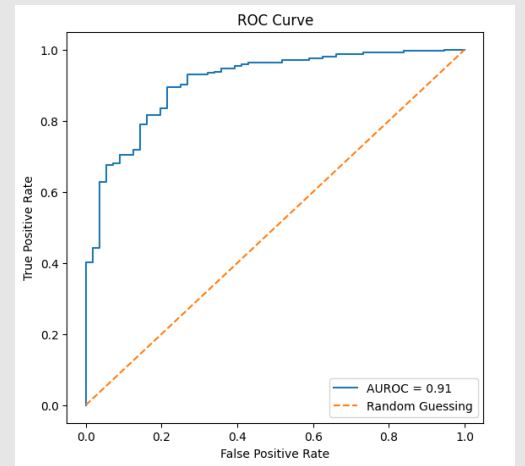
VisA

Dataset	PCB1	PCB2	PCB3	PCB4	Macaronis1	Macaronis2	Analysis	# anomaly classes
PCB1								4
PCB2								4
PCB3								4
PCB4								7
Macaronis1								5
Macaronis2								8
Capsules								7
Candles								7
Cashew								7
Chewing Gum								9
Pipe fryum								6
Fryum								8
								6

Evaluation Metrics

Detection

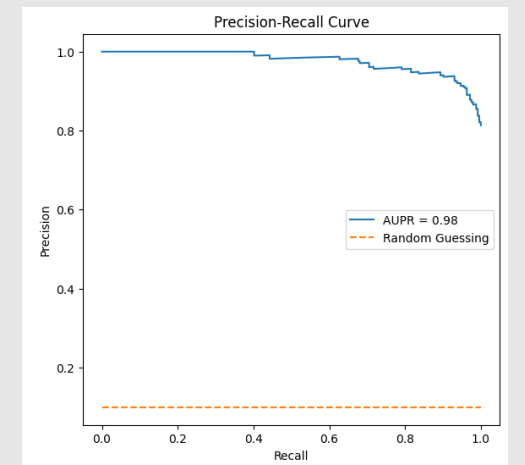
AUROC (Area Under the Receiver Operator Characteristic curve)



AUPR (Area Under the Precision-Recall curve)

Localization

AUPRO (Area Under the Per-Region Overlap)
(Intersection over Union)



Implementation Details

Training

Adam optimizer

Batch size 1 (default)

Learning rate 0.0001 (with step decay schedule)

Image Augmentation

Resizing 256 x 256 pixels & Normalization

ColorJitter (with 0.2 probability)

Hardware

NVIDIA GeForce RTX 3090 GPU (single)

Results and Analysis

Pixel Level

Table 1. Comparison of mean AUPRO scores (%) of current state-of-the-art methods on MVTec AD and VisA datasets.

Method	MVTec AD	VisA
RDAD [7]	93.9	-
S-T [5]	92.4	93.0
FastFlow [47]	92.5	86.8
PatchCore [35]	92.7	79.7
EfficientAD [1]	93.1	93.1
DiffusionAD [50]	-	93.2
FAIR [25]	94.0	91.4
SimpleNet [1]	89.6	68.9
HypAD (Ours)	97.6 (+3.6)	95.4 (+2.2)

Results and Analysis

Pixel Level

Table 2. Pixel-level AUPRO scores (%) of current state-of-the-art methods on MVTec AD dataset. In this table, “texture Mean” and “object Mean” denote the mean of texture and object categories respectively.

	Category	HypAD (Ours)	S-T [5] CVPR 2020	FCDD [26] ICLR 2021	RDAD [7] CVPR 2022	PyramidFlow [21] CVPR 2023	EfficientAD [1] arXiv 2023
texture	carpet	92.7	87.9	99.0	97.0	97.2	91.7
	grid	99.7	95.2	95.0	97.6	-	88.7
	leather	99.9	94.5	99.0	99.1	99.2	98.2
	tile	99.8	94.6	98.0	90.6	97.2	85.8
	wood	95.3	91.1	94.0	90.9	97.9	89.6
texture Mean		97.5	92.7	97.0	95.0	97.9	90.8
object	bottle	100	93.1	96.0	96.6	95.5	95.2
	cable	93.3	81.8	93.0	91.0	90.3	89.9
	capsule	96.9	96.8	95.0	95.8	98.3	97.6
	hazelnut	99.7	96.5	97.0	95.5	98.1	95.1
	metal nut	98.0	94.2	98.0	92.3	-	94.1
	pill	98.4	96.1	97.0	96.4	96.1	96.4
	screw	95.6	94.2	93.0	98.2	-	96.1
	toothbrush	99.9	93.3	95.0	94.5	97.9	94.3
	transistor	100	66.6	90.0	78.0	94.7	91.0
	zipper	94.7	95.1	98.0	95.4	95.4	93.2
object Mean		97.6	90.8	95.2	93.4	95.8	94.3
Mean		97.6	91.4	95.8	93.9	96.5	93.1

Results and Analysis

Pixel Level

Table 3. Pixel-level AUPRO scores (%) of current state-of-the-art methods on VisA dataset.

Category	HypAD (Ours)	S-T [5]	PatchCore [35]	RDAD [7]	DiffusionAD [50]	EfficientAD [1]
		CVPR 2020	CVPR 2022	CVPR 2022	arXiv 2023	arXiv 2023
complex structure	pcb1	97.3	-	94.3	43.2	96.9
	pcb2	98.7	-	89.2	46.4	92.8
	pcb3	97.1	-	90.9	80.3	94.4
	pcb4	97.6	-	90.1	72.2	95.5
multiple instances	candle	94.9	-	94.0	92.2	94.7
	capsules	83.1	-	85.5	56.9	97.6
	macaroni1	98.8	-	95.4	71.3	96.8
	macaroni2	90.2	-	94.4	68.0	98.0
single instance	cashew	95.4	-	94.5	79.0	88.0
	chewing gum	99.6	-	84.6	92.5	87.0
	fryum	93.8	-	85.3	81.0	96.8
	pipe fryum	99.6	-	95.7	68.3	80.2
Mean		95.4	93.0	91.2	70.9	93.2
						93.1

Results and Analysis

MVTec AD Dataset

[Original / GT / Predict Mask / Anomaly Map / Final Result]

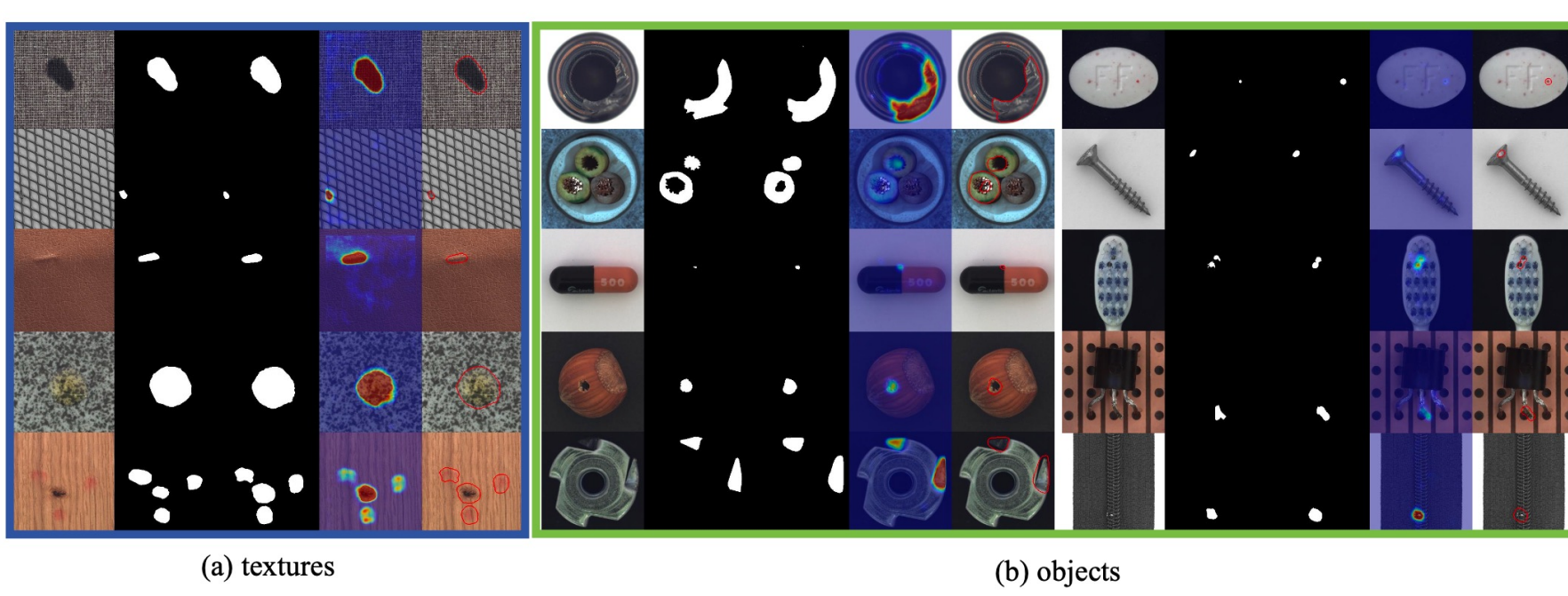
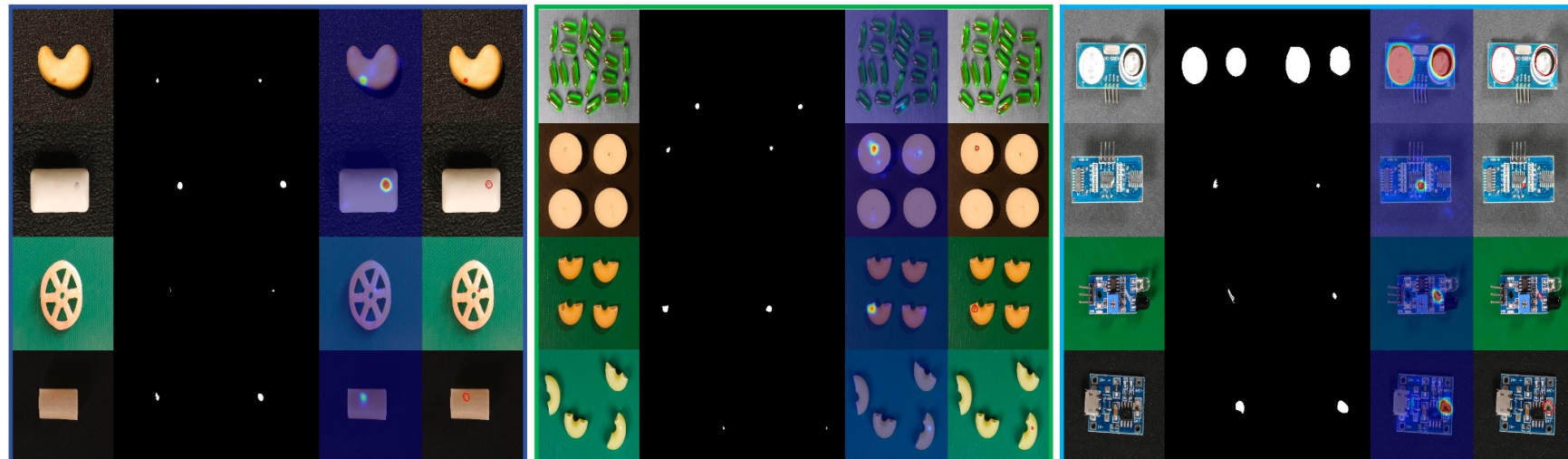


Figure 5. Visualization of each category in MVTec AD. (a) shows five types of texture objects. (b) contains ten categories of objects, three of which (*i.e.* mesh, screw, and zipper) are available only as single-channel images. The visual examples of each class consist of five parts, from left to right are the original image, ground truth, predict mask, anomaly map, and final results. The threshold used by the predict mask is adaptively calculated according to the dataset, without any additional processing.

Results and Analysis

VisA Dataset

[Original / GT / Predict Mask / Anomaly Map / Final Result]



(a) single instance

(b) multiple instance

(c) complex structure

Figure 6. Visualization of each category in VisA. (a) includes four types of single instance. (b) contains four types of multiple instances. (c) contains four types of complex structures. The visual examples of each class consist of five parts, from left to right are the original image, ground truth, predict mask, anomaly map, and final results. The threshold used by the predict mask is adaptively calculated according to the dataset, without any additional processing.

Results and Analysis

Effect of Curvature Parameter c Table 4. Effect of the curvature parameter c in HypAD on VisA.

c	0	0.01	0.05	0.1	0.3	0.5
AUPRO (%)	93.4	95.4	95.2	95.2	95.3	95.3

Results and Analysis

Evaluation on Anomaly Detection (Image Level)

→ Slight improvement, because image-level anomaly detection is relatively simple and its performance has nearly saturated

Further Demonstration on MNIST-C

Table 6. Image-level AUPRO on MNIST-C in ADBench [13].

Method	DevNet [13]	EfficientAD	HypAD
AUROC (%)	88.04	90.96	92.51

Table 5. Comparison (%) of image-level anomaly detection of various methods on MVTec and VisA datasets.

Method	MVTec AD		VisA	
	AUROC	AUPR	AUROC	AUPR
DRA [8]	95.9	-	-	-
MKD [38]	87.7	-	-	-
SPD [51]	94.6	97.5	87.8	88.6
RDAD [7]	98.5	-	-	-
PatchCore [35]	98.7	98.9	94.3	95.2
SoftPatch [19]	98.6	-	-	-
FAIR [25]	98.6	-	96.7	-
EfficientAD [1]	99.0	98.7	97.6	97.5
DiffusionAD [50]	-	-	97.8	-
SimpleNet [1]	98.2	98.5	87.9	90.1
HypAD (Ours)	99.2	99.5	98.3	98.5

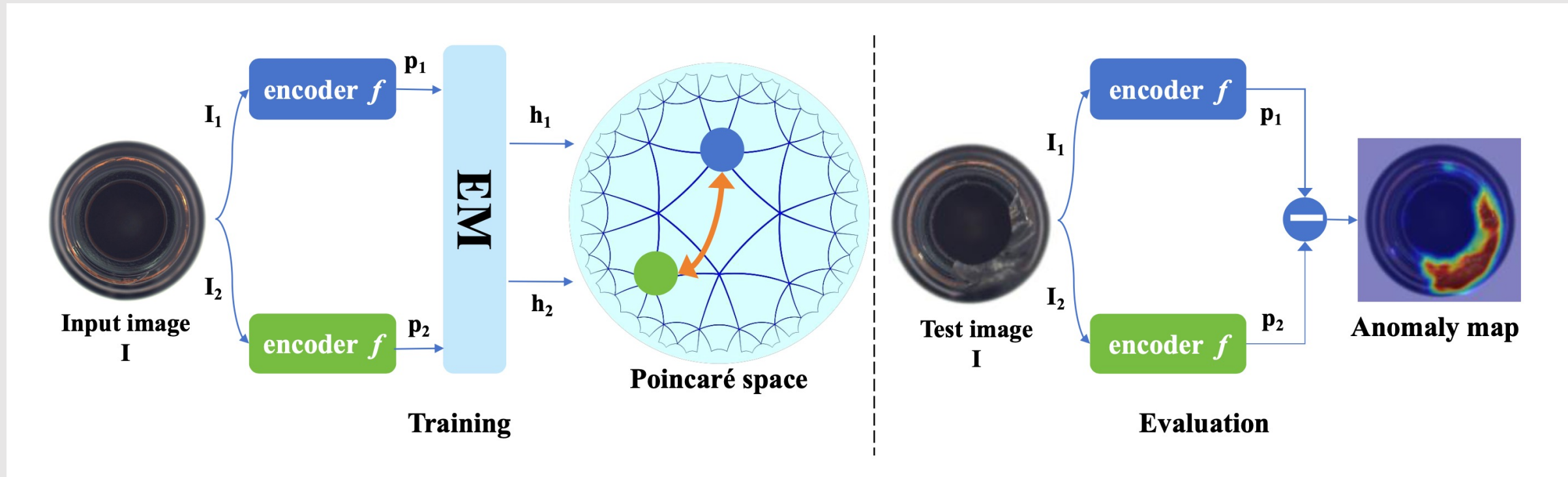
Results and Analysis

Table 7. Comparison (%) of pixel-level AUROC and AUPR of different methods on MVTec and VisA datasets.

Method	MVTec AD		VisA	
	AUROC	AUPR	AUROC	AUPR
MKD [38]	90.7	-	-	-
RDAD [7]	97.8	-	-	-
FAIR [25]	98.2	-	98.8	-
FCDD [26]	96.0	-	-	-
PatchCore [35]	98.1	57.6	94.7	27.8
SoftPatch [19]	97.9	-	-	-
EfficientAD [1]	96.8	60.8	98.9	38.2
SimpleNet [1]	97.1	51.4	91.8	22.6
HypAD (Ours)	98.0	62.5	99.1	37.6

HypAD

Anomaly Detection on Hyperbolic Space(Poincaré ball model)



HypAD

Anomaly Detection on Hyperbolic Space(Poincare ball model)

Table 4. Effect of the curvature parameter c in HypAD on VisA.

c	0	0.01	0.05	0.1	0.3	0.5
AUPRO (%)	93.4	95.4	95.2	95.2	95.3	95.3

HypAD

Anomaly Detection on Hyperbolic Space(Poincare ball model)

- We are the first to explore defect detection problem in hyperbolic space, and present a hyperbolic anomaly detection approach, in which the hyperbolic distance metric is utilized to measure the distance between feature representations.
- Extensive experimental results on the MVTec AD and VisA benchmarks show that our HypAD method achieves state-of-the-art performance, which verifies the advantage of our method and the potential of developing anomaly detection via hyperbolic space.

Thank You